Liquid-Crystalline Complexes of Mesogenic Dimers Containing Oxyethylene Moieties with $LiCF_3SO_3$: Self-Organized Ion Conductive Materials

Toshihiro Ohtake,[†] Masumi Ogasawara,[†] Kaori Ito-Akita,[‡] Naoko Nishina,[‡] Seiji Ujiie,[§] Hiroyuki Ohno,[‡] and Takashi Kato*,[†]

Department of Chemistry and Biotechnology, Graduate School of Engineering, The University of Tokyo, Hongo, Bunkyo-ku, Tokyo 113-8656, Japan; Department of Biotechnology, Tokyo University of Agriculture and Technology, Koganei, Tokyo 184-8588, Japan; and Department of Material Science, Shimane University, Matsue, Shimane 690-8504, Japan

Received November 5, 1999. Revised Manuscript Received January 3, 2000

Mesomorphic dimeric compounds consisting of rigid mesogenic cores and flexible oxyethylene chains have been prepared as liquid-crystalline materials capable of complexing with ionic species. The incorporation of $LiCF_3SO_3$ into these materials results in the induction of smectic A phases and significant mesophase stabilization. The ion−dipole interactions between lithium ions and oxyethylene moieties have stabilized the mesomorphic layer structures. Ionic conductivities have been measured for the complexes forming homeotropically aligned molecular orientation of smectic phases. The highest value of conduction, which is observed for the direction parallel to the layer in the smectic A phase, is 5.5×10^{-4} S cm^{-1}. These results suggest that the complexes of $LiCF_3SO_3$ with mesogenic rod−coil−rod molecules containing oxyethylene chains can function as self-organized ion conductive materials.

Introduction

Liquid crystals are functional materials forming self-organized anisotropic structures.[1] The use of specific molecular interactions, e.g., ion−dipole interactions[2−7] as well as hydrogen-bonding,[8] ionic,[9] and charge-transfer interactions[10] can lead to the formation of a wide variety of dynamically functional supramolecular materials. For example, alkali metal salts were complexed with rod−coil molecules containing oxyethylene chains.[4,5] Cylindrical supramolecular structures were built by the self-assembly of taper-shaped molecules and alkali metal salts.[3] In these cases, the formation of stabilized mesophases was attributed to ion−dipole interactions between metal ions and oxyethylene moieties. Aza-crown and crown ethers attached to mesogenic units function as interacting parts with metal ions, which results in the formation of stable mesophases.[7]

On the other hand, complexes of poly(ethylene oxide)s and alkali metal salts can transport ionic species, which have attracted much attention as solid polymer electrolytes.[11−18] Recently, a variety of ion conductive polymers such as dicharged,[13] hyperbranched,[14] and comb-shaped[15] polymers have been studied. Moreover, the use of the unique nature of liquid crystals, which is dynamic and anisotropic, is expected to lead to the formation of anisotropic mass- or charge-transporting materials.[16−20]

[†] The University of Tokyo.
[‡] Tokyo University of Agriculture and Technology.
[§] Shimane University.

(1) Demus, D., Goodby, J. W., Gray, G. W., Spiess, H. W., Vill, V., Eds. *Handbook of Liquid Crystals*; Wiley-VCH: Weinheim, 1998.
(2) Percec, V.; Johansson, G.; Rodenhouse, R. *Macromolecules* **1992**, *25*, 2563.
(3) Percec, V.; Tomazos, D.; Heck, J.; Blackwell, H.; Ungar, G. *J. Chem. Soc., Perkin Trans. 2* **1994**, 31.
(4) Lee, M.; Oh, N.-K.; Lee, H.-K.; Zin, W.-C. *Macromolecules* **1996**, *29*, 5567.
(5) Lee, M.; Cho, B.-K. *Chem. Mater.* **1998**, *10*, 1894.
(6) (a) Percec, V.; Tomazos, D. *J. Mater. Chem.* **1993**, *3*, 633. (b) Percec, V.; Tomazos, D. *J. Mater. Chem.* **1993**, *3*, 643.
(7) (a) Goodby, J. W.; Mehl, G. H.; Saez, I. M.; Tuffin, R. P.; Mackenzie, G.; Auzély-Velty, R.; Benvegnu, T.; Plusquellec, D. *Chem. Commun.* **1998**, 2057. (b) Shinkai, S.; Nishi, T.; Ikeda, A.; Matsuda, T.; Shimamoto, K.; Manabe, O. *J. Chem. Soc., Chem. Commun.* **1990**, 303.
(8) (a) Kato, T. In *Handbook of Liquid Crystals*; Demus, D., Goodby, J. W., Gray, G. W., Spiess, H. W., Vill, V., Eds.; Wiley-VCH: Weinheim, 1998; Vol. 2B, p 969. (b) Kato, T. *Struct. Bond.* **2000**, *96*, 95. (c) Paleos, C. M.; Tsiourvas, D. *Angew. Chem., Int. Ed. Engl.* **1995**, *34*, 1696.
(9) (a) Hessel, V.; Ringsdorf, H.; Festag, R.; Wendorff, J. H. *Makromol. Chem., Rapid Commun.* **1993**, *14*, 707. (b) Ujiie, S.; Iimura, K. *Chem. Lett.* **1994**, 17. (c) Bazuin, C. G.; Tork, A. *Macromolecules* **1995**, *28*, 8877.
(10) (a) Bengs, H.; Renkel, R.; Ringsdorf, H.; Baehr, C.; Ebert, M.; Wendorff, J. H. *Makromol. Chem., Rapid Commun.* **1991**, *12*, 439. (b) Praefcke, K.; Singer, D.; Kohne, B.; Ebert, M.; Liebmann, A.; Wendorff, J. H. *Liq. Cryst.* **1991**, *10*, 147.
(11) (a) Wright, P. V. *Br. Polym. J.* **1975**, *7*, 319. (b) Bruce, P. G.; Vincent, C. A. *J. Chem. Soc., Faraday Trans.* **1993**, *89*, 3187. (c) Bruce, P. G., Ed. *Solid State Electrochemistry*; Cambridge University Press: Cambridge, 1997.
(12) Meyer, W. H. *Adv. Mater.* **1998**, *10*, 439.
(13) Ito, K.; Nishina, N.; Ohno, H. *J. Mater. Chem.* **1997**, *7*, 1357.
(14) Hawker, C. J.; Chu, F.; Pomery, P. J.; Hill, D. J. T. *Macromolecules* **1996**, *29*, 3831.
(15) Takebe, Y.; Hochi, K.; Matsuba, T.; Shirota, Y. *J. Mater. Chem.* **1994**, *4*, 599.
(16) (a) McHattie, G. S.; Imrie, C. T.; Ingram, M. D. *Electrochim. Acta* **1998**, *43*, 1151. (b) Imrie, C. T.; Ingram, M. D.; McHattie, G. S. *Adv. Mater.* **1999**, *11*, 832.
(17) (a) Dias, F. B.; Batty, S. V.; Ungar, G.; Voss, J. P.; Wright, P. V. *J. Chem. Soc., Faraday Trans.* **1996**, *92*, 2599. (b) Dias, F. B.; Batty, S. V.; Gupta, A.; Ungar, G.; Voss, J. P.; Wright, P. V. *Electrochim. Acta* **1998**, *43*, 1217.
(18) Hubbard, H. V. St. A.; Sills, S. A.; Davies, G. R.; McIntyre, J. E.; Ward, I. M. *Electrochim. Acta* **1998**, *43*, 1239.

10.1021/cm990706w CCC: $19.00
Published on Web 02/29/2000

Chart 1

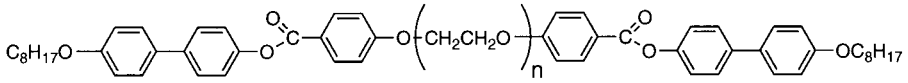

1a: n ≅ 9
1b: n ≅ 13

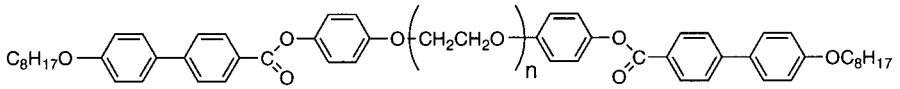

2a: n ≅ 9
2b: n ≅ 13

As for the transport of electrons or holes,[19] photocurrent and carrier mobilities were examined for liquid-crystalline materials.

Our intention is to incorporate ion−dipole interactions for molecular self-organization of liquid crystals as a route to the fabrication of dynamically functional materials such as ion conductive materials. We have designed and synthesized mesomorphic dimeric molecules containing two mesogenic units connected by oxyethylene spacers. Dimeric molecules have been studied intensively not only as model compounds of main-chain liquid-crystalline polymers but also as compounds that show interesting properties.[21,22] Dimeric molecules are expected to be a new class of self-assembled molecular systems.

Here we report significant mesophase stabilization of lithium salt complexes of dimeric mesogenic molecules containing oxyethylene spacers (Chart 1). Ion conduction behavior has been examined for these self-organized mesomorphic materials, forming stable homeotropic monodomains and nonoriented polydomains.

Results and Discussion

The dimeric mesogenic molecules reported here have a rod−coil−rod structure (Chart 1). The rodlike moieties consist of the biphenylene and the phenylene units connected by the ester groups. The oxyethylene chains have been introduced as flexible coil moieties and points of interaction with a lithium salt. Schemes 1 and 2 outline the syntheses of mesogenic dimeric molecules **1** and **2**, respectively. Commercially available poly(ethylene glycol)s with average degrees of polymerization of 9 and 13 were used as starting materials, which were converted to corresponding ditosylates.[23] Compounds **1a** and **1b** were obtained by esterification of **5a** and **5b** with compound **6**, respectively. Substitution reaction of **3a** and **3b** with ethyl 4-hydroxybenzoate and subsequent hydrolysis of the resulting compounds gave compounds **5a** and **5b**, respectively.[24] Compounds **2a** and **2b** were obtained from the reaction of **8a** and **8b** with **11** in chloroform in the presence of dicyclohexylcarbodiimide (DCC) and *N*,*N*-(dimethylamino)pyridine (DMAP). Substitution reaction of **3a** and **3b** with 4-benzyloxyphenol and deprotection of the resulting compounds gave **8a** and **8b**.

Table 1. Thermal Properties of Mesogenic Dimeric Compounds

compound	phase transition behavior[a]										
1a	G	−45	S^b	82 (6.8)	S^b	90 (17.7)	S_C	121 (11.1)	N	135 (2.1)	I
1b					G	−61	S^b	86 (31.1)	N	100 (2.7)	I
2a	G	−46	S^b	57 (5.7)	S_E	77 (3.8)	S_B	121 (5.4)	S_A	170 (11.1)	I
2b	G	−46	S^b	54 (8.1)	S_E	69 (3.2)	S_B	109 (5.4)	S_A	138 (11.9)	I

[a] Transition temperatures (°C) and enthalpies of transition (J/g) on heating. G: glassy; S: smectic; N: nematic; I: isotropic. [b] Unidentified ordered smectic phases.

All dimeric compounds **1a**,**b** and **2a**,**b** show mesomorphic phases. Thermal properties of these compounds are listed in Table 1. Compounds **1a** and **1b** show nematic (N), smectic C (S_C), and ordered smectic phases. In contrast, compounds **2a** and **2b** exhibit smectic A, B, and E phases (S_A, S_B, and S_E) and an ordered smectic phase. No nematic phase is seen for **2a** and **2b**. The direction of the ester linking groups changes the steric effect or polarity of the mesogenic core, which affects the mesomorphism. Such effects were observed for some mesogenic aromatic compounds.[25] With the aid of a microscope, homeotropic alignment can be observed in S_A phases for **2a** and **2b**. Compounds with a shorter oxyethylene spacer ($n \cong 9$) exhibit higher isotropization temperatures (T_i).

Lithium salt complexes of these dimeric compounds were prepared by slow evaporation of the THF solution of dimeric compounds and requisite amounts of $LiCF_3SO_3$. The incorporation of the lithium salt induces significant effects on the mesomorphic behavior of the complexes by ion−dipole interactions. The smectic mesophases are thermally stabilized and the glass transition temperatures increase as the concentration of the salt increases. Table 2 presents the thermal behavior of lithium salt complexes containing 0.3 mol of $LiCF_3$-

(19) (a) Adam, D.; Schuhmacher, P.; Simmerer, J.; Häussling, L.; Siemensmeyer, K.; Etzbach, K. H.; Ringsdorf, H.; Haarer, D. *Nature* **1994**, *371*, 141. (b) Funahashi, M.; Hanna, J. *Phys. Rev. Lett.* **1997**, *78*, 2184. (c) Boden, N.; Bushby, R. J.; Clements, J. *J. Chem. Phys.* **1993**, 98, 5920. (d) Shimizu, Y.; Higashiyama, T.; Fuchita, T. *Thin Solid Films* **1998**, 331, 279.

(20) Ohtake, T.; Ito, K.; Nishina, N.; Kihara, H.; Ohno, H.; Kato, T. *Polym. J.* **1999**, *31*, 1155.

(21) (a) Griffin, A. C.; Britt, T. R. *J. Am. Chem. Soc.* **1981**, *103*, 4957. (b) Jin, J.-I.; Oh, H.-T.; Park, J.-H. *J. Chem. Soc., Perkin Trans. 2* **1986**, 343. (c) Niori, T.; Adachi, S.; Watanabe, J. *Liq. Cryst.* **1995**, *19*, 139. (d) Yoshizawa, A.; Matsuzawa, K.; Nishiyama, I. *J. Mater. Chem.* **1995**, *5*, 2131. (e) Tamaoki, N.; Parfenov, A. V.; Masaki, A.; Matsuda, H. *Adv. Mater.* **1997**, *9*, 1102.

(22) Imrie, C. T. *Struct. Bond.* **1999**, *95*, 149.

(23) Ouchi, M.; Inoue, Y.; Liu, Y.; Nagamune, S.; Nakamura, S.; Wada, K.; Hakushi, T. *Bull. Chem. Soc. Jpn.* **1990**, *63*, 1260.

(24) Kihara, H.; Kato, T.; Uryu, T.; Fréchet, J. M. J. *Chem. Mater.* **1996**, *8*, 961.

(25) (a) Patel, J. S.; Goodby, J. W. *Mol. Cryst. Liq. Cryst.* **1987**, *144*, 117. (b) Goodby, J. W.; Walton, C. R. *Mol. Cryst. Liq. Cryst.* **1985**, *122*, 219. (c) Coates, D.; Gray, G. W. *Mol. Cryst. Liq. Cryst.* **1976**, *37*, 249.

Scheme 1

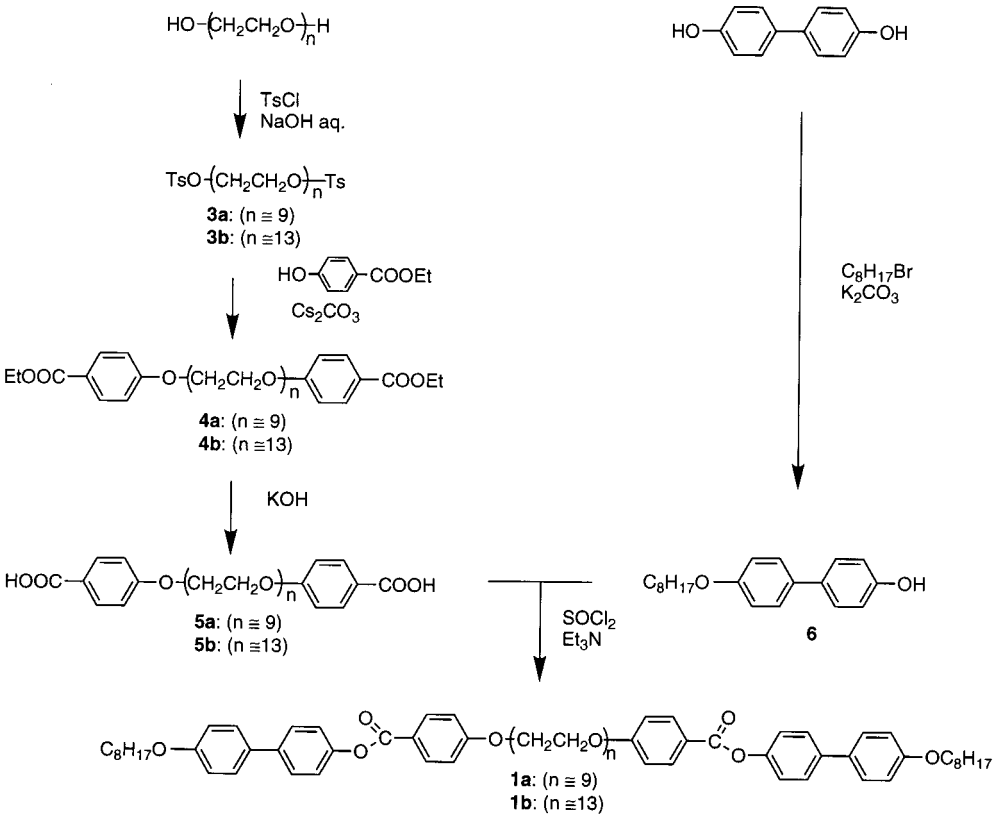

Scheme 2

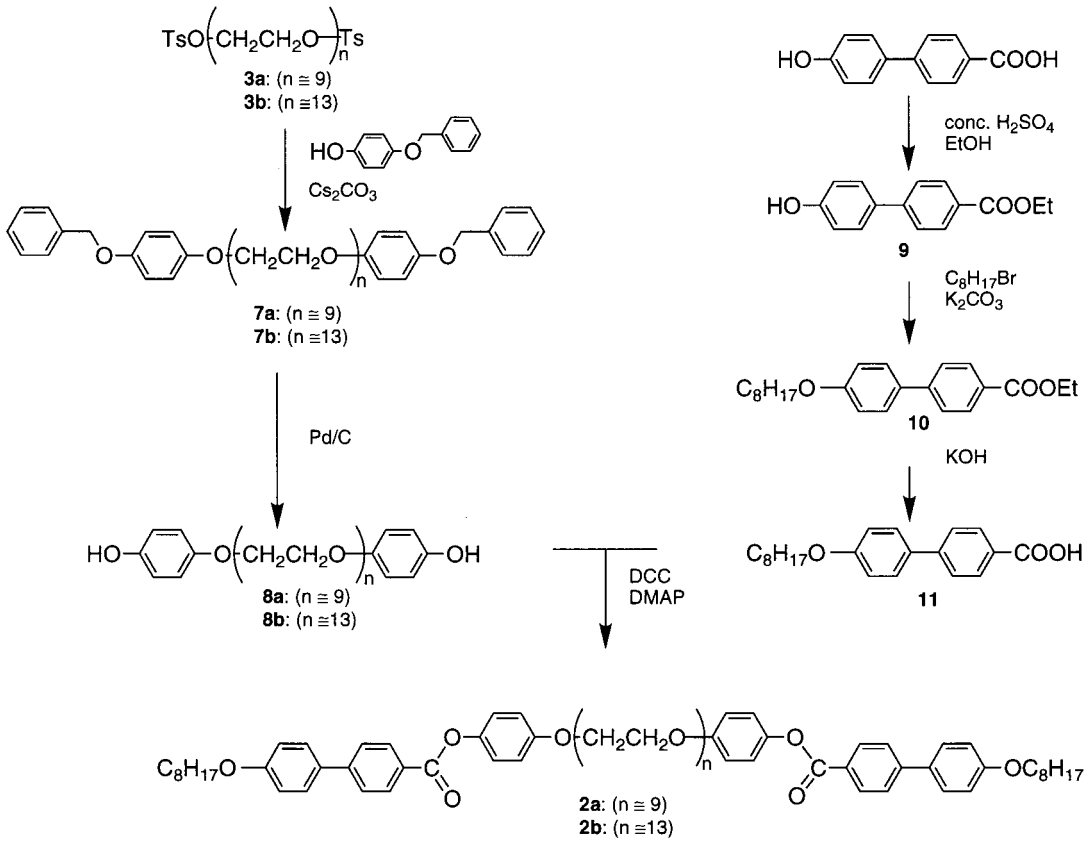

SO_3 per oxyethylene unit. Figure 1 shows the phase diagrams of the complexes of **1a** and **1b** as a function of lithium salt concentration. The incorporation of $LiCF_3SO_3$ into **1a** induces an S_A phase, while only nematic, smectic C, and an unidentified ordered smectic phases are observed for **1a** alone. The isotropization temperature increases from 135 °C for the single component to 186 °C for the complex based on **1a**

Table 2. Thermal Properties of Lithium Salt Complexes of Mesogenic Dimeric Compounds

complex[b]	phase transition behavior[a]						
1a/$LiCF_3SO_3$	G	29	S^c	106 (3.2)	S_A	181 (2.7)	I
1b/$LiCF_3SO_3$	G	21	S^c	79 (1.7)	S_A	144 (2.7)	I
2a/$LiCF_3SO_3$	G	34	S_B	112 (3.2)	S_A	213 (8.3)	I
2b/$LiCF_3SO_3$	G	26	S_B	90 (2.0)	S_A	186 (5.8)	I

[a] Transition temperatures (°C) and enthalpies of transition (J/g) on heating. G: glassy; S: smectic; N: nematic; I: isotropic. [b] Lithium salt concentration: $Li/CH_2CH_2O = 0.3$. [c] Unidentified ordered smectic phases.

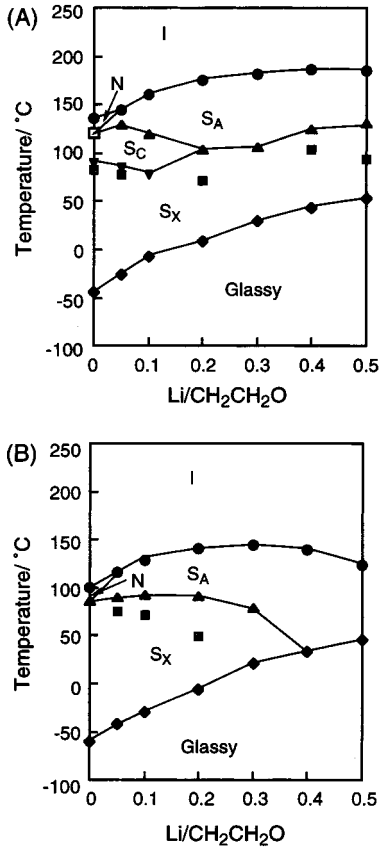

Figure 1. Dependence of the phase transition temperatures of (A) **1a** and (B) **1b** as a function of the molar ratio of the lithium ion to the CH_2CH_2O unit (Li/CH_2CH_2O) on heating (S_X: unidentified smectic phase).

containing 0.4 mol of $LiCF_3SO_3$. The complexes of **1b** also exhibit thermally stabilized S_A phases. The highest T_i is seen at the complex with 0.3 mol of the salt. Figure 2 compares the DSC thermograms of complex **1b** and its single component. Although the phase transition peaks become broader for the complex as shown in Figure 2B, they still show appreciable phase transitions.

Similar transition behavior is observed for the lithium salt complexes of **2a** and **2b**. Figure 3 shows the plot of phase-transition temperatures of complexes **2a** and **2b** as a function of lithium salt concentration. For both compounds, the transition temperatures increase with the increase of the salt concentration. The maximum values of T_i are observed at 216 and 186 °C for **2a** and **2b**, respectively. The degrees of the positive deviation of T_i for both compounds are about 50 °C.

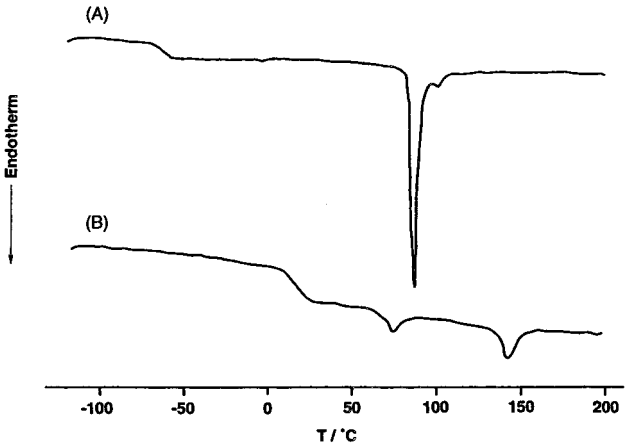

Figure 2. DSC thermograms of (A) **1b** and (B) a lithium salt complex of **1b** ($Li/CH_2CH_2O = 0.3$) on heating.

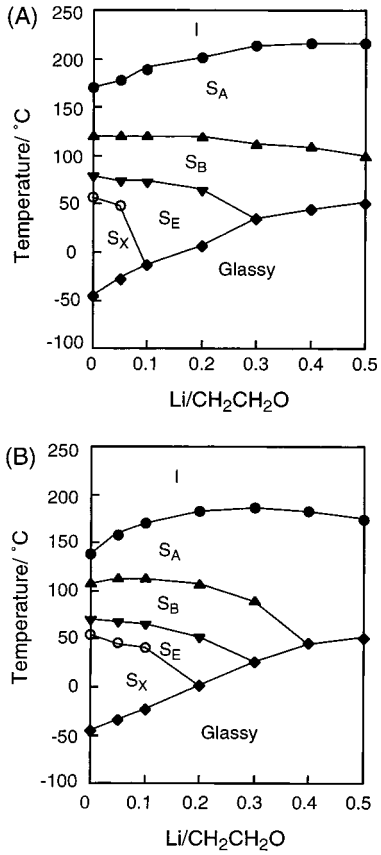

Figure 3. Dependence of the phase transition temperatures of (A) **2a** and (B) **2b** as a function of the molar ratio of the lithium ion to the CH_2CH_2O unit (Li/CH_2CH_2O) on heating (S_X: unidentified smectic phase).

We reported mesomorphic properties of the analogous dimeric compounds of **1**, having pentoxy terminal groups.[20] In this case, no significant stabilization of a smectic A phase was observed. These results suggest that terminal alkyl chains also function as important parts for the stabilization of the S_A phase.

The observation that the glass transition temperatures increase with the addition of the lithium salt (Figures 1 and 3) suggests that lithium salts intermolecularly interact with oxyethylene moieties by ion−dipole interactions. Lithium salt complexes of the dimeric compounds, having the longer oxyethylene chain, give lower isotropization temperatures.

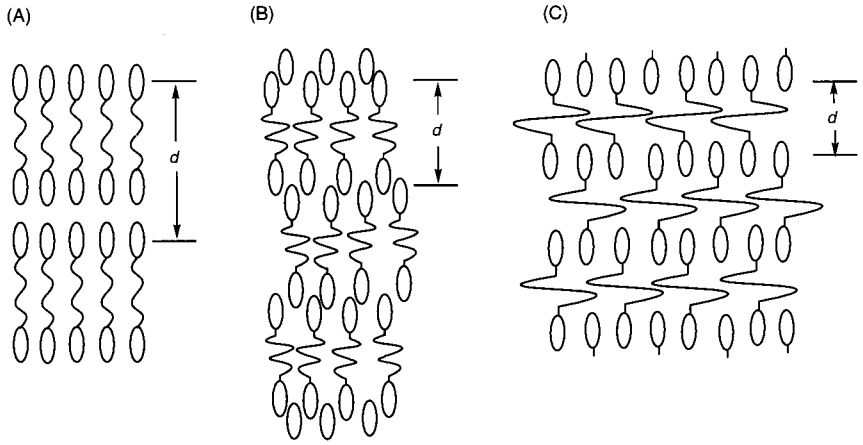

Figure 4. Schematic illustrations of packing structures of the dimer complexes in S_A phases: (A) bilayer structure of **1a** and **1b**; (B) partially interdigitated bilayer structure of **2a**; and (C) monolayer structure of **2b**.

Table 3. Layer Spacings of the Complexes[a] of Mesogenic Dimeric Compounds in Smectic A Phases

complex	T,[b] °C	layer spacing d, Å
1a/$LiCF_3SO_3$	130	75
1b/$LiCF_3SO_3$	110	76
2a/$LiCF_3SO_3$	140	41
2b/$LiCF_3SO_3$	130	23

[a] Lithium salt concentrations are $Li/CH_2CH_2O = 0.05$. [b] All temperatures reported are for the cooling run.

Recently, lithium salt complexes of rod−coil molecules were shown to exhibit a stabilized mesophase.[4,5] The induction of thermally stable S_A phases or columnar phases was observed. The degree of the positive deviation for the S_A phase was about 20 °C.[4] On the other hand, for the rod−coil−rod dimeric molecules prepared in the present work, lateral interactions between mesogenic cores on both sides lead to the significant stabilization of the smectic layer structures of the complexes.

X-ray diffraction studies have been performed for the complexes containing $LiCF_3SO_3$, which can be used as self-organized ion conductive materials. Table 3 lists the layer spacings of these complexes in S_A phases. The complexes of **1a**,**b** give larger layer spacings compared with those of complexes **2a**,**b**. Possible models for these smectic layer structures are illustrated in Figure 4. The complexes of **1a** and **1b** may form bilayer molecular packing (Figure 4A). The molecular packing of complex **2a** may be a partially interdigitated bilayer structure (Figure 4B). It is noteworthy that the layer spacing observed for the complex of **2b** is 23 Å. This smaller spacing suggests that the complex exhibits a monolayer smectic phase (Figure 4C).[22] Figure 5 shows the comparison of X-ray diffraction patterns of salt-free **2b** and **2b**'s lithium salt complex. The layer spacing drastically decreases from 44 to 23 Å when complexed with $LiCF_3SO_3$. The interaction of the lithium salt with the oxyethylene chain of **2b** may introduce a more coiled structure of the spacer (Figure 4C), which may be due to the formation of an ionic domain. This conformational change results in the decrease of the thickness of the oxyethylene layer and the formation of the monolayer smectic phase. The mesogenic core of **2b** may also favor this molecular arrangement.

Ionic conductivities have been measured for the lithium salt complexes of mesomorphic dimeric molecules **2a** and **2b**. Figure 6 schematically illustrates the structures of two types of cells employed for conductivity measurements. Cell A consists of a glass plate on which gold is deposited to form a comb shape. The width of tooth and the thickness of gold electrode are 0.3 mm and 0.8 μm, respectively. On the other hand, for cell B, a pair of indium tin oxide (ITO) electrodes is employed. The thickness between two electrodes is fixed by Teflon spacer to be 20 μm. The salt concentration of the complexes for the measurements is 0.05 mol per oxyethylene unit. The samples were placed in the electrodes and heated to isotropization temperatures. The cell was then gradually cooled to an ambient temperature. For cell A, the complex can spontaneously form an oriented homeotropic monodomain, which is revealed by conoscope observation (Figure 7). In contrast, for cell B, a fan-shaped texture has been observed on the ITO electrode, indicating the formation of polydomain alignment. The ionic conductivities for complexes **2a** and **2b** are presented in Figure 8. Ionic conductivities perpendicular to the molecular director of the smectic layer have been measured for the oriented monodomain sample in comb-shaped electrodes. The ionic conductivities of complex **2b** are higher than those of complex **2a**, which has a shorter oxyethylene chain. The highest conductivity achieved for complex **2b** is 5.5×10^{-4} S cm^{-1} in the smectic A phase at 152 °C. In the S_A phase,

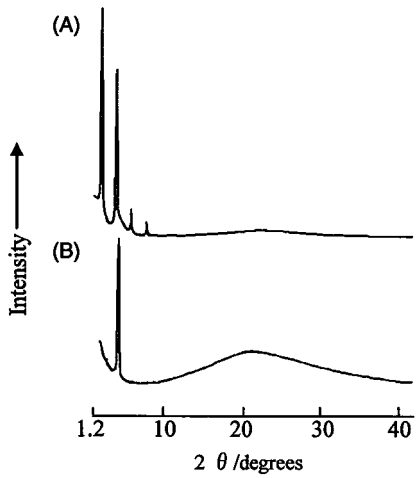

Figure 5. X-ray diffraction patterns of (A) **2b** that is free of salt and (B) a lithium salt complex of **2b** ($Li/CH_2CH_2O = 0.05$) in S_A phases at 130 °C.

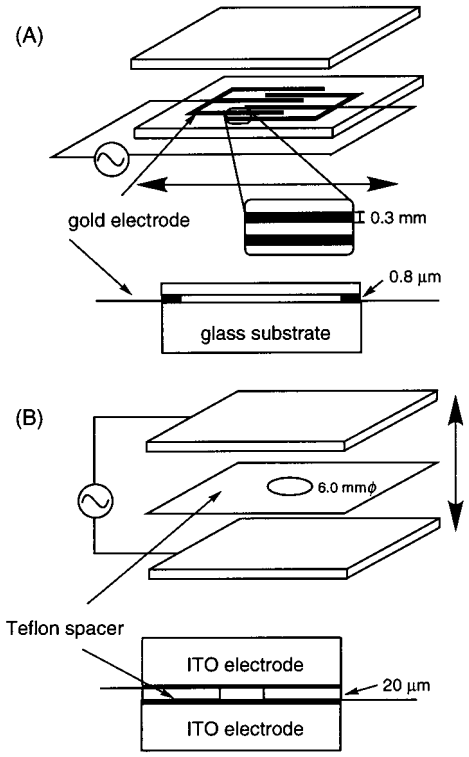

Figure 6. Schematic view of the cells used for conductivity measurements: (A) comb-shaped gold electrodes and (B) ITO electrodes. The arrows show the direction of conductivity measurements.

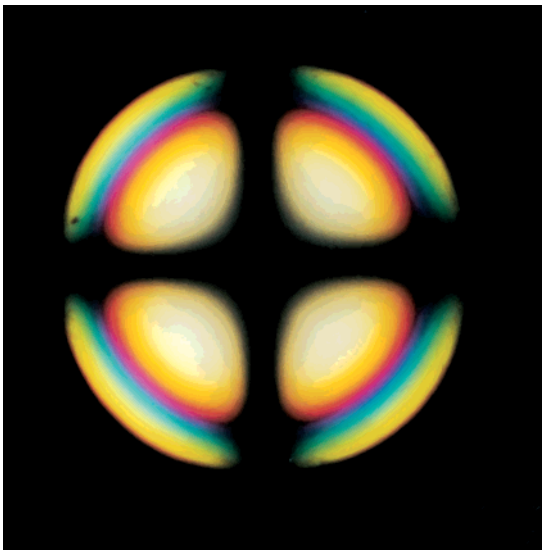

Figure 7. Conoscopic figure observed for the homeotropically aligned lithium salt complex of **2b** ($Li/CH_2CH_2O = 0.05$) in an S_A phase.

ionic conductivities become higher than those observed for the isotropic liquid. These results suggest that ionic species can be transported faster in the homeotropically oriented smectic layer than in the isotropic liquid. Moreover, in the smectic B phase at 97 °C, the conductivity is 1.9×10^{-4} S cm^{-1}, which is comparable to that observed for amorphous poly(oxyethylene) materials containing the same amount of the salt (3.1×10^{-4} S cm^{-1}).[26] X-ray results have suggested that even in

(26) Alloin, F.; Sanchez, J.-Y.; Armand, M. *J. Electrochem. Soc.* **1994**, *141*, 1915.

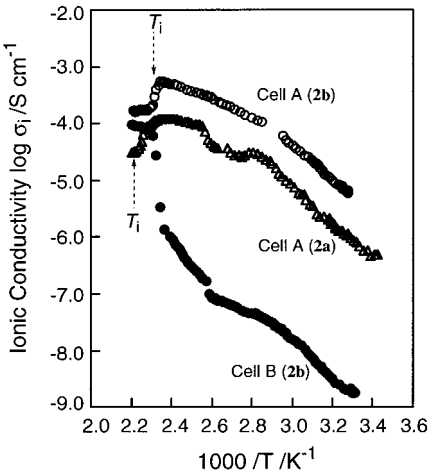

Figure 8. Ionic conductivities of lithium salt complexes of **2a** and **2b** ($Li/CH_2CH_2O = 0.05$): (○) homeotropically aligned monodomain sample of complex **2b** in cell A; (△) homeotropically aligned monodomain sample of complex **2a** in cell A; (●) unaligned polydomain sample of complex **2b** in cell B.

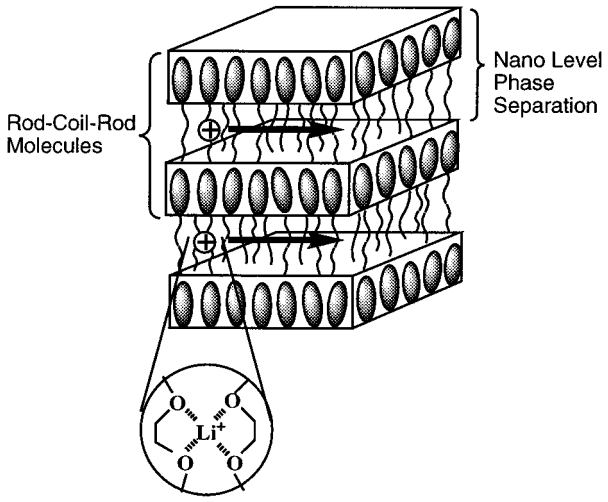

Figure 9. Schematic representation of ion conduction for the complex of the mesogenic dimer and the lithium salt in the cell A in Figure 6A.

smectic phases significant random conformation of the oxyethylene spacer exists for complex **2b.** Such nanolevel phase separation of the ordered region of the mesogenic moieties and the amorphous region of the random ionic coil of the oxyethylene moieties might contribute to the high ionic conductivities of the materials. For the polydomain sample of complex **2b**, the conductivities drastically decrease in the smectic A phase because of the formation of a polydomain structure which disturbs the arrangement of ion paths.

The dimeric mesogenic compounds reported here can provide a monodomain of a stable smectic layer structure as schematically illustrated in Figure 9. In this structure, nanolevel phase separation of the layer of the oriented mesogens and the random ionic layer induces anisotropic ion conduction. The self-organized materials of mesogenic salt complexes should provide us with a novel architecture for ion conductive materials.

Experimental Section

Materials. Unless otherwise noted, the reagents and solvents were purchased from Aldrich or Tokyo Kasei and used as received.

Characterization. ^{1}H NMR spectra were measured on a JEOL JNM-EX270 FT NMR spectrometer at 270 MHz or on a JEOL JNM-LA400 FT NMR spectrometer at 400 MHz. Chemical shifts of the signal were quoted relative to $(CH_3)_4Si$ ($\delta = 0.00$) as an internal standard. The following abbreviations are used to explain the multiplicity: s = singlet, d = doublet, t = triplet, q = quartet, and m = multiplet. FT-IR measurements were conducted on a JASCO FT/IR-8900μ spectrometer. DSC measurements were performed on a Mettler DSC 30. Heating and cooling rates were 10 °C min^{-1}. The transition temperatures were taken at the maximum of exothermic and minimum point of endothermic peaks, respectively. The midpoint of the change in the heat capacity was taken as a glass transition temperature. A polarizing microscope (Olympus BH-2) equipped with a hot stage (Mettler FP82HT) and crossed polarizers was used for visual observations. X-ray diffraction patterns were measured with a Rigaku RINT 2100 diffractometer.

α,ω-Bis(*p*-toluenesulfonyl)oligo(oxyethylene)s (3a,b). Synthesis of **3a**: To the mixture of a THF (5 mL) solution of poly(ethylene glycol) ($M_w \cong 400$) (22 g, 55 mmol) and a 24% NaOH aqueous solution (15 mL) in an ice bath was added dropwise a THF (15 mL) solution of *p*-toluenesulfonyl chloride (22 g, 0.11 mol) with continuous stirring at 0 °C. The resulting mixture was stirred at 0 °C for 2 h. The solution was then poured into ice water. The aqueous solution was extracted with three portions of chloroform. The combined organic extracts were dried with anhydrous $MgSO_4$, filtered, and concentrated in vacuo. The residue was purified by column chromatography (silica gel; eluent was chloroform followed by chloroform/methanol = 20/1) to give **3a** (38 g, 54 mmol) in 97% yield as a colorless oil. ^{1}H NMR ($CDCl_3$, 270 MHz): $\delta = 2.45$ (s, 6 H), 3.58−3.73 (m, 32 H), 4.16 (t, $J = 5$ Hz, 4 H), 7.35 (d, $J = 8$ Hz, 4 H), 7.80 (d, $J = 8$ Hz, 4 H). Compound **3b**: Yield, 67%.

α,ω-Bis(4-ethoxycarbonylphenyl)oligo(oxyethylene)s (4a,b). Synthesis of **4a**: A mixture of **3a** (18 g, 25 mmol), ethyl 4-hydroxybenzoate (8.5 g, 51 mmol), and Cs_2CO_3 (19 g, 59 mmol) in DMF (100 mL) was stirred at room temperature for 72 h under an N_2 atmosphere. DMF was then removed under reduced pressure, and the residue was washed thoroughly with chloroform. The organic solution was washed with water and brine, dried over anhydrous $MgSO_4$, and filtered. The solvent was evaporated, and the crude product was purified by column chromatography (silica gel; eluent was hexane/ethyl acetate = 3/1 followed by chloroform/methanol = 20/1) to give **4a** (17 g, 48 mmol) in 95% yield as a pale yellow oil. ^{1}H NMR ($CDCl_3$, 270 MHz): $\delta = 1.38$ (t, $J = 7$ Hz, 6 H), 3.57−3.72 (m, 28 H), 3.87 (t, $J = 5$ Hz, 4 H), 4.18 (t, $J = 5$ Hz, 4 H), 4.34 (q, $J = 7$ Hz, 4 H), 6.92 (d, $J = 9$ Hz, 4 H), 7.98 (d, $J = 9$ Hz, 4 H). Compound **4b**: Yield, 73%.

α,ω-Bis(4-carboxyphenyl)oligo(oxyethylene)s (5a,b). Synthesis of **5a**: A solution of **4a** (17 g, 24 mmol) and KOH (5.0 g, 89 mmol) in ethanol (120 mL) was refluxed for 7 h. The solution was poured into water, acidified by diluted HCl, and extracted with chloroform. The organic layer was washed with water, dried over anhydrous $MgSO_4$, filtered, and evaporated to give **5a** (12 g, 18 mmol) in 77% yield as white waxy solids: mp 51 °C (DSC on second heating). ^{1}H NMR ($CDCl_3$, 270 MHz): $\delta = 3.62$−3.73 (m, 28 H), 3.88 (t, $J = 5$ Hz, 4 H), 4.21 (t, $J = 5$ Hz, 4 H), 6.95 (d, $J = 9$ Hz, 4 H), 8.02 (d, $J = 9$ Hz, 4 H). Compound **5b**: Yield, 90%; mp, 41 °C (DSC on second heating).

4-Hydroxy-4′-octyloxybiphenyl (6). A mixture of 4,4′-dihydroxybiphenyl (20 g, 0.11 mol) and K_2CO_3 (7.0 g, 51 mmol) in acetone (150 mL) was refluxed for 0.5 h, and then 1-bromooctane (21 g, 0.11 mol) was added in one portion to the mixture under reflux. The reaction mixture was refluxed for 24 h and then poured into water and acidified with diluted HCl. The precipitate was collected by suction funnel and recrystallized from ethanol to obtain **6** (9.0 g, 33 mmol) in 30% yield as a white powder. Phase transition temperatures (°C): crystal 108 unidentified smectic 148 isotropic (DSC on second heating). ^{1}H NMR ($CDCl_3$, 270 MHz): $\delta = 0.89$ (t, $J = 7$ Hz, 3 H), 1.29−1.85 (m, 12 H), 3.98 (t, $J = 7$ Hz, 2 H), 6.88 (d, $J = 9$ Hz, 2 H), 6.94 (d, $J = 9$ Hz, 2 H), 7.40−7.47 (m, 4 H).

α,ω-Bis(4-benzyloxyphenyl)oligo(oxyethylene)s (7a,b). Synthesis of **7a**: Compound **3a** (8.0 g, 11 mmol), 4-benzyloxyphenol (4.6 g, 23 mmol), and Cs_2CO_3 (14 g, 44 mmol) were placed in DMF (60 mL) and stirred at room temperature for 72 h under an N_2 atmosphere. After removal of the solvent under reduced pressure, the residue was extensively washed with chloroform. The resulting organic solution was washed with water and brine, dried over Na_2SO_4, filtered, and evaporated under reduced pressure. Purification by column chromatography (silica gel; eluent was hexane/ethyl acetate = 3/1 followed by chloroform/methanol = 40/1) of the residue afforded **7a** (6.8 g, 7.9 mmol) in 72% yield as a pale orange oil. ^{1}H NMR ($CDCl_3$, 270 MHz): $\delta = 3.64$−3.73 (m, 28 H), 3.84 (t, $J = 5$ Hz, 4 H), 4.07 (t, $J = 5$ Hz, 4 H), 5.01 (s, 4 H), 6.82−6.91 (m, 8 H), 7.28−7.44 (m, 10 H). Compound **7b**: Yield, 88%.

α,ω-Bis(4-hydroxyphenyl)oligo(oxyethylene)s (8a,b). Synthesis of **8a**: A mixture of **7a** (6.7 g, 8.8 mmol) and 10% Pd/C (0.70 g) in ethyl acetate (100 mL) was vigorously stirred under an H_2 atmosphere with a slightly positive pressure for 15 h. The reaction mixture was filtered through a Celite pad, and the combined filtrate was evaporated. The residue was purified by column chromatography (silica gel; eluent was chloroform/methanol = 20/1) to obtain **8a** (4.5 g, 8.0 mmol) in 91% yield as a yellow oil. ^{1}H NMR ($CDCl_3$, 270 MHz): $\delta = 3.59$−3.78 (m, 28 H), 3.81 (t, $J = 5$ Hz, 4 H), 4.05 (t, $J = 5$ Hz, 4 H), 6.76 (s, 8 H). Compound **8b**: Yield, 85%.

Ethyl 4′-Hydroxy-4-biphenylcarboxylate (9). A solution of 4′-hydroxy-4-biphenylcarboxylic acid (10 g, 47 mmol) and catalytic amounts of concentrated H_2SO_4 in ethanol (150 mL) was refluxed for 18 h. The resulting mixture was poured into water, extracted with chloroform, washed with water and saturated $NaHCO_3$ aqueous solution, and dried over Na_2SO_4. Recrystallization of the residue from hexane/ethyl acetate afforded **9** (10 g, 41 mmol) in 88% yield as a white powder. Mp: 141.0−141.3 °C. ^{1}H NMR ($CDCl_3$, 270 MHz): $\delta = 1.41$ (t, $J = 7$ Hz, 3 H), 4.40 (q, $J = 7$ Hz, 2 H), 5.19 (s, 1 H), 6.94 (d, $J = 9$ Hz, 2 H), 7.50 (d, $J = 9$ Hz, 2 H), 7.60 (d, $J = 9$ Hz, 2 H), 8.08 (d, $J = 9$ Hz, 2 H).

Ethyl 4′-Octyloxy-4-biphenylcarboxylate (10). Compound **9** (10 g, 42 mmol) and K_2CO_3 (9.0 g, 65 mmol) in DMF (100 mL) were heated at 80 °C for 0.5 h before the addition of 1-bromooctane (8.8 g, 46 mmol) in one portion to the solution. The reaction mixture was heated at 120 °C for 22 h under an N_2 atmosphere, and the resulting mixture was poured into water and filtered. The precipitate was collected by suction funnel and dissolved in chloroform. The organic solution was washed with 1 M NaOH aqueous solution and brine, dried over Na_2SO_4, filtered, and evaporated in vacuo. The residue was purified by column chromatography (silica gel; eluent was hexane/ethyl acetate = 7/1) to give **10** (10 g, 29 mmol) in 68% yield as a white powder. Phase transition temperatures (°C): crystal 54 unidentified smectic 70 S_E 82 S_B 92 S_A 109 isotropic (DSC on second heating). ^{1}H NMR ($CDCl_3$, 270 MHz): $\delta = 0.89$ (t, $J = 7$ Hz, 3 H), 1.29−1.55 (m, 13 H), 1.76−1.83 (m, 2 H), 4.00 (t, $J = 7$ Hz, 2 H), 4.39 (q, $J = 7$ Hz, 2 H), 6.98 (d, $J = 9$ Hz, 2 H), 7.56 (d, $J = 9$ Hz, 2 H), 7.61 (d, $J = 8$ Hz, 2 H), 8.08 (d, $J = 8$ Hz, 2 H).

4′-Octyloxy-4-biphenylcarboxylic acid (11). An ethanol (150 mL) solution of compound **10** (10 g, 28 mmol) and KOH (4.0 g, 71 mmol) was refluxed for 6 h. The resulting mixture was poured into water and acidified with diluted HCl. The precipitate was collected by suction funnel. Recrystallization from acetic acid gave **11** (8.3 g, 25 mmol) in 90% yield as white solids. Phase transition temperatures (°C): crystal 182 S_C 252 N 260 isotropic (DSC on second heating). ^{1}H NMR (DMSO-d_6, 270 MHz): $\delta = 0.83$ (t, $J = 7$ Hz, 3 H), 1.24−1.39 (m, 10 H), 1.64−1.75 (m, 2 H), 3.98 (t, $J = 7$ Hz, 2 H), 7.00 (d, $J = 9$ Hz, 2 H), 7.65 (d, $J = 9$ Hz, 2 H), 7.72 (d, $J = 9$ Hz, 2 H), 7.95 (d, $J = 9$ Hz, 2 H), 12.8 (br s, 1 H).

α,ω-Bis{4-[(4′-octyloxy-4-biphenylyl)oxycarbonyl]phenyl}oligo(oxyethylene)s (1a,b). Synthesis of **1a**: Compound **5a** (2.0 g, 3.1 mmol) dissolved in $SOCl_2$ (10 mL) was refluxed for 3 h with stirring before the excess of $SOCl_2$ was removed under reduced pressure. The residue was dissolved in dry THF (5 mL), and the flask was cooled to 0−5 °C by an ice bath.

Compound **6** (1.9 g, 6.4 mmol) and triethylamine (2.5 mL) in dry THF (10 mL) were then added dropwise to the mixture at 0−5 °C. After the resulting mixture was stirred overnight at room temperature, the solvent was evaporated, and the residue was thoroughly washed with chloroform. The combined organic solution was washed with diluted HCl and brine, dried over $MgSO_4$, filtered, and concentrated in vacuo. The crude product was purified by column chromatography (silica gel; eluent was chloroform followed by chloroform/methanol = 20/1) to give **1a** (2.3 g, 1.9 mmol) in 61% yield as white colorless solids. ^{1}H NMR ($CDCl_3$, 400 MHz): δ = 0.89 (t, J = 7 Hz, 6 H), 1.30−1.83 (m, 24 H), 3.64−3.75 (m, 28 H), 3.90 (t, J = 5 Hz, 4 H), 4.00 (t, J = 7 Hz, 4 H), 4.22 (t, J = 5 Hz, 4 H), 6.97 (d, J = 9 Hz, 4 H), 7.01 (d, J = 9 Hz, 4 H), 7.24 (d, J = 8 Hz, 4 H), 7.51 (d, J = 9 Hz, 4 H), 7.58 (d, J = 8 Hz, 4 H), 8.16 (d, J = 9 Hz, 4 H). ^{13}C NMR ($CDCl_3$, 100.5 MHz): δ = 14.0, 22.6, 26.0, 29.2, 29.3, 31.7, 67.6, 68.0, 69.4, 70.5, 70.8, 114.3, 114.7, 121.8, 121.9, 127.6, 128.0, 132.2, 132.7, 138.4, 149.8, 158.6, 163.0, 164.9. IR (KBr): 762, 809, 842, 1087, 1116, 1134, 1221, 1255, 1291, 1499, 1509, 1607, 1734, 2872, 2922 cm^{-1}. Compound **1b**: Yield, 62%.

α,ω-Bis{4-[(4′-octyloxy-4-biphenylyl)carbonyloxy]-phenyl}oligo(oxyethylene)s (2a,b). Synthesis of **2a**: A solution of DCC (1.6 g, 7.8 mmol) in chloroform (20 mL) was added dropwise to a mixture of **8a** (1.8 g, 3.1 mmol), **11** (2.0 g, 6.1 mmol), and DMAP (0.6 g, 4.9 mmol) in chloroform (90 mL) with stirring at 0−5 °C. The mixture then was stirred at room temperature for 72 h under an N_2 atmosphere. Precipitates were removed through a glass filter and washed with chloroform, and the filtrate was evaporated under reduced pressure. The residue was dissolved in chloroform, and the solution was washed with 5% HCl, brine, 1 M NaOH aqueous solution, brine, and water, successively. The organic layer was dried over Na_2SO_4, filtered, and concentrated in vacuo. The residue was purified by column chromatography (silica gel; eluent was chloroform/ethyl acetate = 3/1 followed by chloroform/methanol = 20/1) to give **2a** (2.7 g, 2.3 mmol) in 74% yield as white colorless solids. ^{1}H NMR ($CDCl_3$, 270 MHz): δ = 0.90 (t, J = 7 Hz, 6 H), 1.30−1.70 (m, 20 H), 1.82 (m, 4 H), 3.65−3.74 (m, 28 H), 3.87 (t, J = 5 Hz, 4 H), 4.01 (t, J = 7 Hz, 4 H), 4.14 (t, J = 5 Hz, 4 H), 6.96 (d, J = 9 Hz, 4 H), 7.00 (d, J = 9 Hz, 4 H), 7.13 (d, J = 9 Hz, 4 H), 7.59 (d, J = 9 Hz, 4 H), 7.68 (d, J = 9 Hz, 4 H), 8.22 (d, J = 9 Hz, 4 H). ^{13}C NMR ($CDCl_3$, 100.5 MHz): δ = 14.1, 22.6, 26.0, 29.2, 29.3, 31.7, 67.8, 68.0, 69.6, 70.5, 70.6, 70.8, 114.9, 115.2, 122.4, 126.5, 127.5, 128.3, 130.6, 131.8, 144.5, 145.8, 156.4, 159.5, 165.4. IR (KBr): 766, 832, 816, 948, 1089, 1129, 1202, 1253, 1295, 1508, 1604, 1725, 1732, 2859, 2923 cm^{-1}. Compound **2b**: Yield, 81%.

Measurements of Ionic Conductivity. Dynamic ionic conductivity measurements were performed for cells A and B with an impedance analyzer (Schlumberger, Solartron 1260) and custom setup temperature controller equipped with a computer. The heating rate for the ionic conductivity measurements was 3−5 °C min^{-1}. The samples were placed in the electrodes and heated to isotropization temperatures. Then the cell was gradually cooled to room temperature.

Preparation of Lithium Salt Complexes. All complexes examined in the present study were prepared by slow evaporation from THF solution containing the requisite amounts of $LiCF_3SO_3$ and mesogenic dimeric compounds followed by drying overnight in vacuo at 60 °C.

Acknowledgment. Financial support of Grant-in-Aid for Scientific Research on Priority Areas, “New Polymers and Their Nano-Organized Systems” (277/08246101) from Ministry of Education, Science, Sports, and Culture is gratefully acknowledged. One of the authors (K.I.-A.) appreciates the financial support of Research Fellowship of the Japan Society for the Promotion of Science (JSPS) for Young Scientists.

CM990706W